

# Effect of Poly(ethylene-*co*-glycidyl methacrylate) Compatibilizer Content on the Morphology and Physical Properties of Ethylene Vinyl Acetate–Wood Fiber Composites

D. G. Dikobe, A. S. Luyt

Department of Chemistry, University of the Free State (Qwaqwa Campus), Phuthaditjhaba 9866, South Africa

Received 14 May 2006; accepted 26 December 2006

DOI 10.1002/app.26080

Published online 5 March 2007 in Wiley InterScience (www.interscience.wiley.com).

**ABSTRACT:** In this study, ethylene vinyl acetate (EVA)–wood fiber (WF) (uncompatibilized) and EVA/poly(ethylene-*co*-glycidyl methacrylate) (EGMA)-WF (compatibilized) were blended, and their morphology as well as mechanical, thermal, O<sub>2</sub> permeability, and water absorption properties were investigated. It is shown that there is a possible interaction between EVA and WF. This interaction seems to be very weak, and the resulting composites have poor properties. The presence of EGMA in the composite improved most of the investigated properties. IR analysis shows that there is a grafting reaction between EGMA and WF. The resulting

composites have better properties than EVA or its uncompatibilized composites. The amount of compatibilizer has an effect on the properties of the composites. The mechanical properties improved with increasing EGMA content, but thermal stability decreased with increasing EGMA content. Oxygen permeability and water absorption decreased with an increase in EGMA content in the composites. © 2007 Wiley Periodicals, Inc. *J Appl Polym Sci* 104: 3206–3213, 2007

**Key words:** EVA; EGMA; wood fiber composites; thermal analysis; tensile properties; gas permeability

## INTRODUCTION

Natural fibers, used to fill and reinforce polymers, represent one of the fastest-growing types of polymer additives.<sup>1–3</sup> Natural fiber composites are formulated from a blend of natural fibers, including cane fibers, bamboo, oat, kenaf, hemp, flax, jute and sisal, and wood fiber (WF), and thermoplastic polymers, such as polypropylene and polyesters. The resulting composites are stronger, stiffer, and lightweight, because the natural fibers stop the propagation of cracks in the matrix.<sup>3–7</sup> The polymer matrix provides an environment for the fibers to reside in their original shape and protects them from scratches that might cause them to fracture under low stress. The fibrous filler adds strength to the more fragile polymer material by shouldering much of the stress that was transferred from the polymer to the fiber through their strong interfacial bonds.<sup>8</sup>

WF in particular, due to its low density and availability, has been studied as a polymer reinforcement since the 1980s, and the resulting composites have

been thoroughly investigated and reported.<sup>8–14</sup> WF is obtainable as a waste after plane shaving from wood industries. It has different particle sizes and can therefore produce composites with different properties depending on the particle size used. The resulting WF–polymer composites have high specific mechanical properties.<sup>14,15</sup> WFs, however, do not usually perform satisfactorily as polymer reinforcement, owing to the high percentage of their hydroxyl groups and high surface polarity.<sup>7–9,11,14</sup> In a composite, the efficiency of the filler depends primarily on the capability to transfer the applied stress from the continuous phase (matrix) to the fibers. This is not achieved with WFs, owing to poor adhesion between the hydrophilic surface of the natural fibers and the essentially hydrophobic polymers which are commonly used as the matrix.<sup>5–7</sup> Because the mechanical properties of heterogeneous structures depend on the quality of interfaces between the components, it was crucial to develop additive substances favoring chemical bonds between the fiber and the matrix. Different chemical substances have been used as compatibilizers of wood polymer composites by various researchers.<sup>7,16,17</sup> Salemane and Luyt<sup>16</sup> used maleic anhydride grafted polypropylene (MAPP) as a compatibilizer in WF–PP composites and reported improved properties compared with composites without MAPP. To improve the compatibility between the WF and the LLDPE matrix, Liao et al.<sup>10</sup>

Correspondence to: A. S. Luyt (luytas@qwa.uovs.ac.za).

Contract grant sponsor: National Research Foundation, South Africa; contract grant number: GUN 2050677.

Contract grant sponsor: University of the Free State.

treated the WF with titanate coupling agents or grafted it with acrylonitrile. Both treatments resulted in an improvement in the mechanical properties of the resultant composites compared with the composites filled with the untreated WF. The grafting method displayed more improved mechanical properties than the titanate coupling method. The mechanical properties of compression-molded polystyrenes filled with sawdust wood residue of softwood and hardwood species have been investigated by Maldas et al.<sup>11</sup> To improve the compatibility of the WFs with the polymer matrices, different treatments (e.g., graft copolymerization) and coupling agents (e.g., silanes and isocyanates at various concentrations) were used. The mechanical properties were improved considerably in treated WF–PS composites compared with the untreated ones. The compatibilizing agents become chemically linked to the hydrophilic WF, and facilitate the wetting of the hydrophobic polymer chain. Compatibilizers should therefore have both hydrophobic and hydrophilic characteristics, making bonding between the two constituents much easier.

Another drawback is the high moisture absorption of the WFs. Moisture absorption can result in swelling of the fibers, and concerns on the stability of the fiber composites cannot be ignored.<sup>7</sup> The absorption of moisture by the fibers is minimized in the composite because of encapsulation by the polymer. Moisture absorption of the fibers can be dramatically reduced through chemical modification of some of the hydroxyl groups present in the fiber, but with some increase in the cost of the fiber. Good fiber-matrix bonding can also decrease the rate and amount of water absorbed by the composite.<sup>18</sup> Espert et al.<sup>19</sup> reported that mechanical properties were dramatically affected by water absorption in composites without compatibilizer, and less water was absorbed when ethylene vinyl acetate (EVA) was used as a compatibilizer for WF–PP composites. Elvy et al.<sup>20</sup> reported that the usage of coupling agents decreased the strand between the polymer and the cell wall of the wood and therefore resulted in reduction in water absorption.

Very little has been reported on EVA–natural fiber composites. Malunka et al.<sup>17</sup> investigated EVA–sisal fiber composites in the absence and presence of dicumyl peroxide (DCP), which initiated crosslinking, and reported DCP to be effective in grafting EVA to sisal fiber resulting in composites with better physical properties. Sedlakova et al.<sup>21</sup> reported the ability of poly(ethylene-*co*-methacrylic acid) copolymer (EMAA) to effectively compatibilize low-density polyethylene–WF composites. Both the mechanical and dynamic mechanical results showed that EMAA promotes better interaction between LDPE and WF. A high content of WF and low content of EMAA in

the system yield materials with high modulus and high tensile strength. These studies showed the effectiveness of methacrylate based copolymers as compatibilizers for polymer–natural fiber composites.

For this study, poly(ethylene-*co*-glycidyl methacrylate) (EGMA), another methacrylate acid copolymer, was used as a compatibilizer in EVA–WF composites. The effect of EGMA compatibilizer content on the morphology, mechanical, thermal, and water absorption properties of EVA–WF composites were investigated.

## MATERIALS AND METHODS

EVA copolymer with 9% vinyl acetate (VA) content was used as the composite matrix. It has a density of 0.93 g cm<sup>-3</sup>, a melting point of 95°C, a tensile strength of 19 MPa, and a 750% elongation at break. EGMA was used as a compatibilizer. It has a density of 0.93 g cm<sup>-3</sup>, a melting point of 93°C, a tensile strength of 12 MPa, and an elongation at break of 440%. Both polymers were supplied by Plastamid, Elsie River, South Africa.

Pine WF, or pine saw dust, was obtained from FBW Taurus, Phuthaditjhaba, South Africa. It was supplied as a light orange-colored-powder with a density of 1.5 g cm<sup>-3</sup>. WF particles (<150 μm) were obtained by sieving the received WF using laboratory test sieves of 150 μm pore size. It has an aspect ratio of ~ 1 and a maximum specific surface area of ~ 7 × 10<sup>5</sup> μm<sup>2</sup>.

Samples were weighed according to the required ratios to make up a total of 40 g (which is the mass required for thoroughly mixing the different components in the Brabender mixer). Mixing of the samples was done at a temperature of 130°C and a mixing speed of 30 min<sup>-1</sup> for 15 min. The samples were then melt pressed at 120°C and 100 bar for 5 min. Pressed samples were allowed to cool at room temperature for 10 min before touching them to avoid air from penetrating, which will promote the formation of bubbles.

The morphology of EVA–WF composites were examined by means of a polarized optical microscope. A very thin film of the sample was placed on a glass slide, and polarized optical photos were taken at 100× magnification using a CETI polarized optical microscope made in Belgium. The photos were taken with a Ceist DCM digital camera.

IR analyses were done on a Nicolet Magna 550 FTIR spectrophotometer (Nicolet Instruments, Madison). Samples were prepared by mixing the composite (±3 mg) with dry KBr (±300 mg). The mixture was pressed in a die under high pressure to prepare a pellet. The pellet was scanned in the region of 400–4000 cm<sup>-1</sup> at a resolution of 4 cm<sup>-1</sup>.

DSC analyses were carried out on a Perkin–Elmer DSC7 differential scanning calorimeter (Wellesley, Massachusetts) under flowing nitrogen ( $20 \text{ mL min}^{-1}$ ). The samples with a mass of  $\pm 7.5 \text{ mg}$  were heated from  $25$  to  $150^\circ\text{C}$  at a rate of  $20^\circ\text{C min}^{-1}$ , held at  $25^\circ\text{C}$  for  $1 \text{ min}$  to eliminate thermal history, cooled to  $25^\circ\text{C}$ , and reheated under the same conditions. The melting and crystallization data were obtained from the second scan.

TGA analyses were carried out using a Perkin–Elmer TGA7 thermogravimetric analyzer (Wellesley, Massachusetts). Samples of mass  $\pm 10 \text{ mg}$  were heated from  $50$  to  $600^\circ\text{C}$  at a heating rate of  $20^\circ\text{C min}^{-1}$  under flowing nitrogen ( $20 \text{ mL min}^{-1}$ ).

Tensile properties were determined using a Hounsfield H5KS (Hounsfield Test Equipment, Redhill, England) tensile tester. At least eight dumbbell samples, with a gauge length of  $24 \text{ mm}$ , width of  $5 \text{ mm}$ , and thickness of  $1 \text{ mm}$ , of each composite were analyzed at a speed of  $50 \text{ mm min}^{-1}$ .

To determine the gas permeability of the composite samples, oxygen was supplied at different flow rates, and the analyses were done using a Sierra Smart-Trak mass flow meter (Sierra Instruments, California).

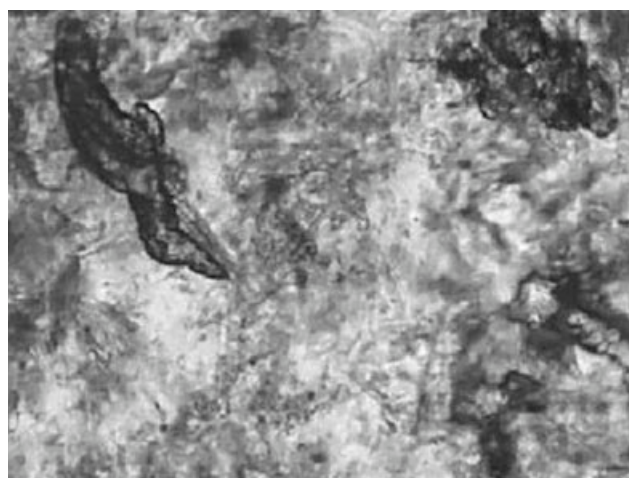
For water absorption determinations, samples were cut into  $30 \text{ mm} \times 20 \text{ mm}$  sheets. Samples were dried at  $70^\circ\text{C}$  to reach constant weight. The samples were then immersed into a static distilled water bath at room temperature. Water uptake at time  $t$  of the composites was calculated using eq. (1).

$$\% \text{ water uptake} = (M_t - M_0)/M_0 \times 100 \quad (1)$$

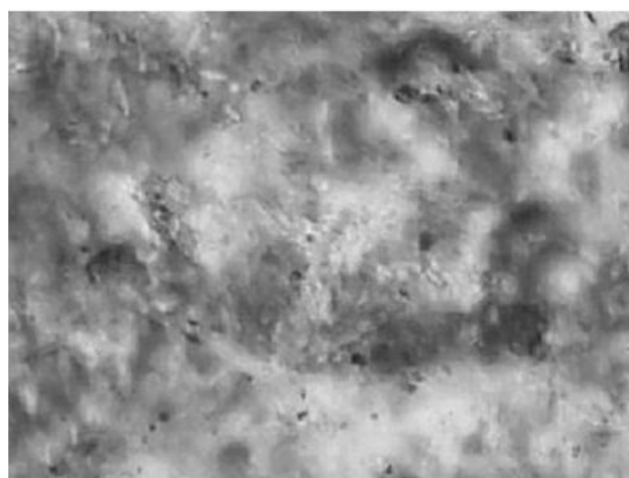
where  $M_t$  is the mass of the sample at time  $t$  and  $M_0$  is the mass of the sample before insertion into the water. Samples were immersed in water for  $72 \text{ h}$  and water uptake measurements were recorded at  $24 \text{ h}$  intervals. The water uptake was plotted as a function of time.

## RESULTS AND DISCUSSION

The effect of the compatibilizer on the physical appearance of the composites can be compared by looking at the photos in Figure 1. The degree of dispersion of the WF in the matrix in the  $95/0/5 \text{ w/w}$  EVA/EGMA–WF composite is restricted [Fig. 1(a)]. The composite does not show homogeneity. This is because of the incompatibility between WF and EVA. Although EVA contains acetate polar groups that could interact with hydrophilic cellulosic fibers, compatibility is not fully favorable because of the EVA polymer backbone that is hydrophobic and thus tends to repel WF. The  $90/5/5 \text{ w/w}$  EVA/EGMA–WF ( $<150 \mu\text{m}$ ) composite shows a better dispersion of the WF particles in the matrix [Fig. 1(b)].



(a)



(b)



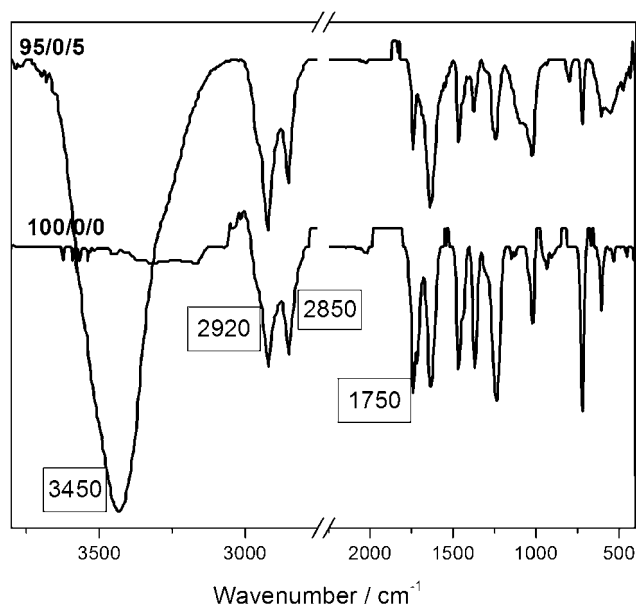
(c)

**Figure 1** Polarized optical microscopy photos ( $\times 100$  magnification) of EVA/EGMA–WF ( $<150 \mu\text{m}$ ) composites: (a)  $95/0/5 \text{ w/w}$ ; (b)  $90/5/5 \text{ w/w}$ ; and (c)  $85/10/5 \text{ w/w}$ .

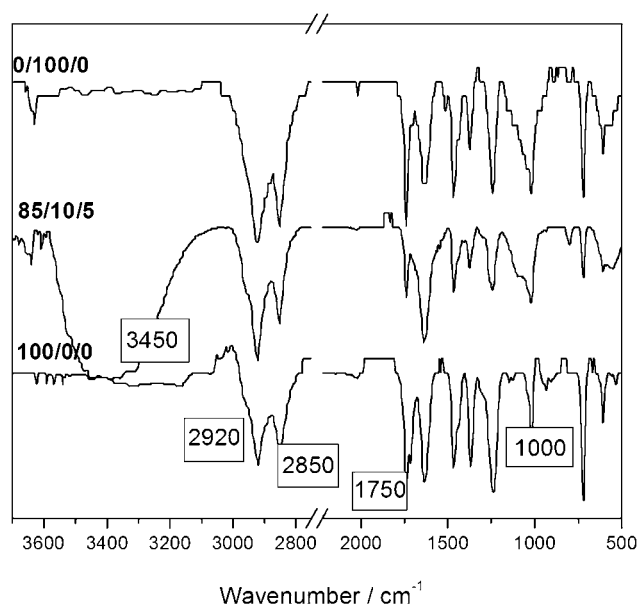
There is a better interaction between the polymer matrix and the WF particles. The reason for this is that EGMA reacts with WF, decreasing its surface energy and its hydrophilicity (see discussion below). When 10% of compatibilizer was used in the 85/10/5 w/w EVA/EGMA-WF composite [Fig. 1(c)], compatibility between the WF particles and the polymer is improved. The composite shows homogeneity, adhesion is better, and the surface of the composite is smooth in comparison with the uncompatibilized and 5% compatibilized composites. This shows that the compatibilizer promotes interfacial adhesion between EVA and WF.

Figure 2 shows the infrared spectra of pure EVA and EVA-WF composites. The spectrum of pure EVA presents peaks around 2850 and 2920  $\text{cm}^{-1}$  that represent C-H vibrations. The peak representing the vibration of the  $-\text{C}=\text{O}$  ester of the carboxyl group appears at 1750  $\text{cm}^{-1}$ . When 5% WF is present in the composite, a large peak at 3450  $\text{cm}^{-1}$  is seen, indicating the presence of OH groups. The other peaks that were seen in pure EVA are still present. The intensities of the peaks around 2850 and 2920  $\text{cm}^{-1}$  increase, which indicates that the WF contains C-H groups. The presence of the peak at 1750  $\text{cm}^{-1}$  indicates that the  $-\text{C}=\text{O}$  content remains the same in the composite. There is therefore no grafting reaction between EVA and WF, but there may be hydrogen bonding between the  $-\text{OH}$  groups on the cellulose and the  $-\text{C}=\text{O}$  groups in the vinyl acetate.

The 85/10/5 w/w EVA/EGMA-WF composite shows a broad peak around 3450  $\text{cm}^{-1}$  indicating the presence of OH groups. For EGMA, peaks are seen at 2850 and 2920  $\text{cm}^{-1}$ , indicating C-H vibra-



**Figure 2** IR spectra of pure EVA and EVA-WF composites.



**Figure 3** IR spectra of pure EVA, pure EGMA, and an EVA/EGMA-WF composite.

tions (Fig. 3). Peaks are seen at 1750  $\text{cm}^{-1}$  for  $-\text{C}=\text{O}$  and at 1000  $\text{cm}^{-1}$  for the epoxy group. The characteristic peaks of EGMA and EVA are still seen in this composite spectrum. The peak at 1750  $\text{cm}^{-1}$  is still visible, which shows that the final product consists of  $-\text{C}=\text{O}$  functional groups. The intensity of the peak at 1000  $\text{cm}^{-1}$ , representing the epoxy group, has decreased compared with that of pure EGMA. Reaction between the epoxy group in EGMA and the carboxyl group in EVA is highly unlikely. Reaction between the epoxy group of EGMA and an OH group in WF is more likely, and such a reaction is well known and has been extensively reported.<sup>22–25</sup> The fact that there is a decrease in this peak intensity indicates that there is a possible reaction between EGMA and WF. The peak at 1750  $\text{cm}^{-1}$  does not disappear completely because the resulting composite still contains  $-\text{C}=\text{O}$  functional groups. It is further clear from Figure 3 that, for compatibilized composites, the OH peak at 3450  $\text{cm}^{-1}$  is greatly reduced compared with the  $-\text{OH}$  peak for the uncompatibilized composite (Fig. 2). This is not only because of the EGMA-WF reaction, but probably also because of epoxy hydrolysis, which is likely to occur to a certain extent, because epoxy containing compounds or polymers are known to act as acid or water scavengers, thus reducing the number of  $-\text{OH}$  groups in the composite.<sup>23</sup> Wetting of the WF surface by grafted EGMA, combined with good EVA-EGMA miscibility (see discussion below), should cause improved matrix-WF interaction, leading to improved physical properties.

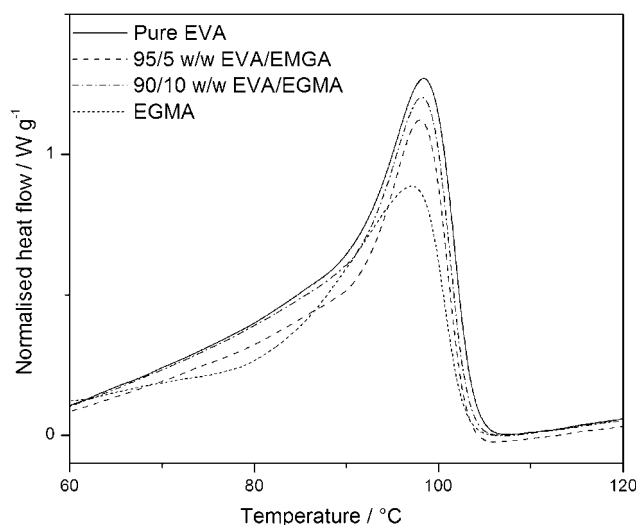


**Figure 4** DSC heating curves of pure EVA and EVA/EGMA blends.

Chiou et al.<sup>23</sup> investigated *in situ* compatibilized PP/liquid crystalline polymer blends (LCP), and reported that the epoxy functional group of the EGMA copolymer can react with the carboxylic acid and/or the hydroxyl end groups of the LCP. Heino and Seppala<sup>22</sup> investigated an ethylene-ethyl acrylate-glycidyl methacrylate (E-EA-GMA) terpolymer as a reactive compatibilizer for PP/LCP blends, and they suggested that the reaction/interaction between PP and LCP was because of the epoxy group of E-EA-GMA. Chiou et al.<sup>24</sup> reported styrene-glycidyl methacrylate (SGMA) as an effective reactive compatibilizer for polystyrene/LCP blends. The epoxy functional group in the SGMA reacted with the carboxylic acid or hydroxyl end groups during melt processing. Miller et al.<sup>25</sup> used PP functionalized acrylic acid (PP-AA) as a compatibilizer for PP/LCP and, based on the observed compatibilization effect, concluded that there appears to be an interaction between the polar acrylic acid groups and the LCP rather than a true covalent bond.

Figure 4 shows that pure EGMA and EVA have melting peaks in the same temperature range. As discussed above, there is no evidence of a reaction taking place between EVA and EGMA. According to Chiou et al.,<sup>23</sup> a reaction with EGMA is likely to occur with those polymers containing certain functional groups as chain ends or within the main chain. Typical examples are  $-\text{COOH}$  (and/or  $-\text{OH}$ ) of polyesters, phenolic  $-\text{OH}$  of PPO, and  $\text{NH}_2$  of polyamides. Looking at the structure of EVA, none of these functional groups are present at the chain end or within the main chain, so that there is no probability of EVA and EGMA forming a reactive product during melt extrusion. The single melting peak for the blends, as well as the relative peak

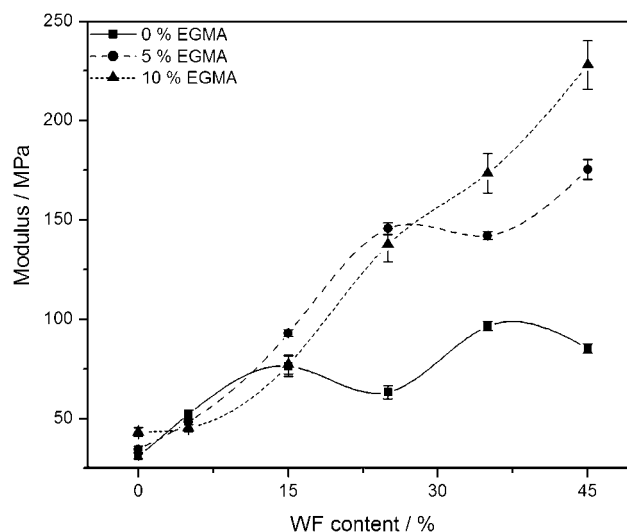


**Figure 5** Effect of EGMA content on the tensile modulus of EVA/EGMA-WF (<150  $\mu\text{m}$ ) composites.

sizes, therefore show that EVA and EGMA are miscible in the crystalline phase, and do not substantially influence each other's crystallization behavior. The decrease in enthalpy with increasing EGMA content is the result of the lower melting enthalpy of EGMA (Fig. 4).

The influence of WF and EGMA contents on the mechanical properties of the composites are shown by the modulus, stress at break, and elongation at break curves in Figures 5–7. EGMA has a higher modulus than EVA, so that EVA/EGMA blends are expected to have higher moduli than pure EVA. The 10% EGMA compatibilized composites have higher Young's modulus values than the 5% EGMA compatibilized and uncompatibilized composites (Fig. 5). The presence of WF in pure EVA and in EVA/EGMA

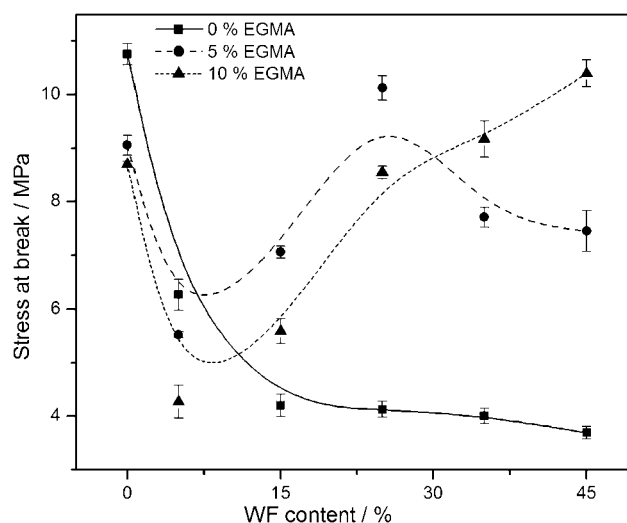


**Figure 6** Effect of EGMA content on the stress at break of EVA/EGMA-WF (<150  $\mu\text{m}$ ) composites.

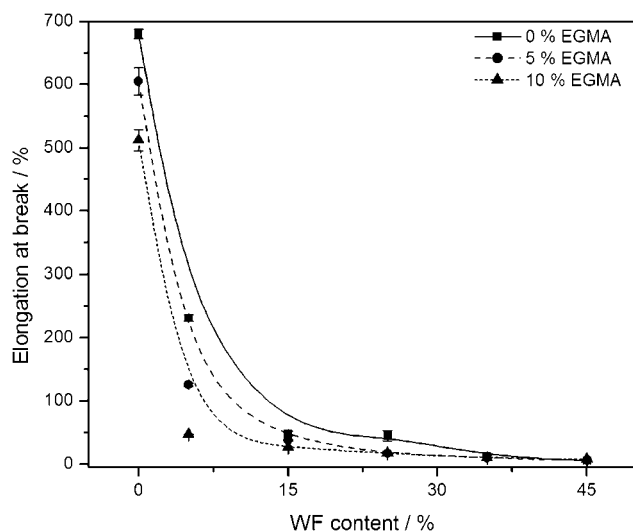


**Figure 7** Effect of EGMA content on the elongation at break of EVA/EGMA-WF (<150  $\mu\text{m}$ ) composites.

blends causes an increase in modulus, although the increase in the case of pure EVA is only marginal. The reason is probably a fairly weak interaction between EVA and WF in the absence of EGMA. The amount of EGMA does not seem to make a difference at low WF content, while at high WF content the modulus increases faster with increasing WF content in the presence of 10% EGMA than in the presence of 5% EGMA content. This is probably because of the increased number of active groups available to react with WF. Salemane and Luyt<sup>16</sup> reported that the use of a compatibilizer improved the adhesion and tensile properties of PP-WF composites. The composite properties changed with an increase in maleated polypropylene (MAPP) content. This improved filler-matrix interfacial adhesion is probably due to an esterification reaction between the hydroxyl groups of the cellulose filler and the anhydride functionalities of MAPP. Malunka et al.<sup>17</sup> reported that increasing sisal content as well as crosslinking and grafting gave rise to increased values of Young's modulus.

The effect of compatibilizer and WF contents on the stress at break of the composites is shown in Figure 6. Pure EVA has a tensile strength of 11 MPa. The presence of 5 and 10% EGMA in the EVA causes a decrease in tensile strength to 9 and 8.5 MPa, respectively. There is a continuous decrease in tensile strength as more WF is present in the uncompatibilized composites. Ismail and Jaffri<sup>15</sup> reported that the inability of the filler to support stresses transferred from the polymer matrix, increases with increase in filler loading. Georgopoulos et al.<sup>5</sup> studied thermoplastic polymers reinforced with fibrous agricultural residue, and they reported a significant decrease in tensile stress upon filling the polymer

matrix with natural fillers. Stress at break values increase with increasing WF content above 5% when EGMA is used as a compatibilizer. For 5% EGMA, the stress at break decreases again at high filler loading and for 10% EGMA there is a continuous increase after an initial decrease. The initial decrease is probably due to the small amount of WF, which does not provide enough  $-\text{OH}$  groups to react with epoxy groups in EGMA. The decrease at high WF content in the presence of 5% EGMA is probably because there is not enough EGMA to completely react with the WF surfaces, giving rise to reduced interaction with EVA.

The effect of EGMA and WF contents on the elongation at break of the composites is shown in Figure 7. Pure EVA has an elongation at break of 680%, and the presence of 5 and 10% EGMA in EVA causes a decrease 600 and 500%, respectively. This is the result of the lower chain mobility of EGMA. The presence of WF causes a sharp decrease in elongation at break, with the uncompatibilized composites having somewhat lower values than the compatibilized ones. Georgopoulos et al.<sup>5</sup> also reported a decrease in elongation at break; the matrix/filler composite seems to lose most of its flexibility, even at lower filler loading. The composites with 35 and 45% WF show an insignificant difference in elongation at break, irrespective of whether the composites are compatibilized or not.

The presence of EGMA causes a decrease in gas permeability compared with pure EVA (Fig. 8). WF reduces the gas permeability of EVA, even in the absence of EGMA. This shows that WF accommodates amorphous EVA chains in their pores, giving rise to lower  $\text{O}_2$  permeability values. The presence of EGMA and WF remarkably reduces

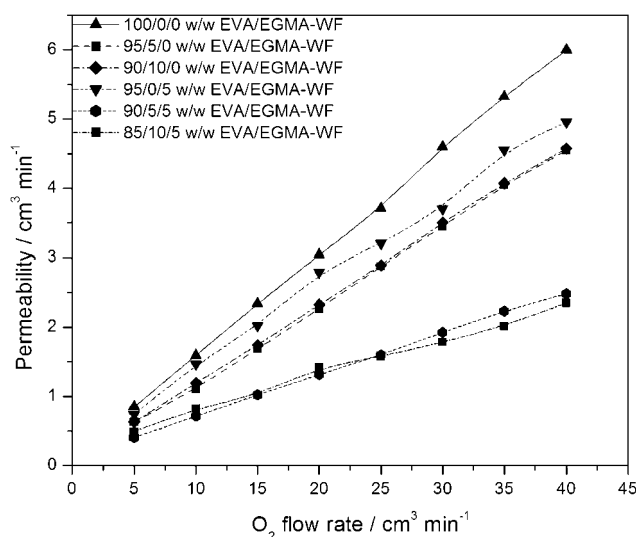


**Figure 8** Permeability of samples as function of oxygen flow rate.

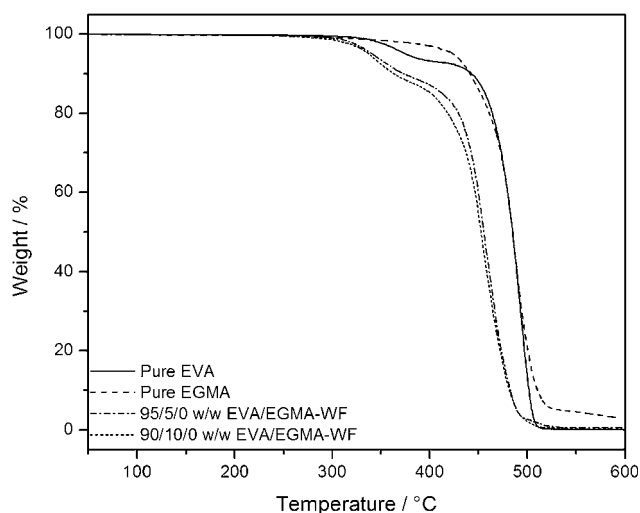


**Figure 9** TGA curves of pure EVA and EVA/EGMA blends.

the  $O_2$  permeability of the composites. This is because of the strong interfacial adhesion between WF and EVA/EGMA, resulting in composites that are less porous and less amorphous than the uncompatibilized EVA composites.

The TGA curves of EVA and EVA/EGMA blends are shown in Figure 9. The EVA/EGMA blends have two degradation steps just like pure EVA, with the onset of degradation at lower temperatures than those of pure EVA and pure EGMA. The reason for this reduction in the onset temperature of degradation is the presence of EGMA, which starts degrading at a lower temperature than EVA, thus negatively affecting the degradation temperature of the EVA/EGMA blends. The TGA curves of the composites, when 25% of WF is used, are shown in Figure 10. Both the first and second degradation steps in the uncompatibilized composites occur at higher temperatures than those

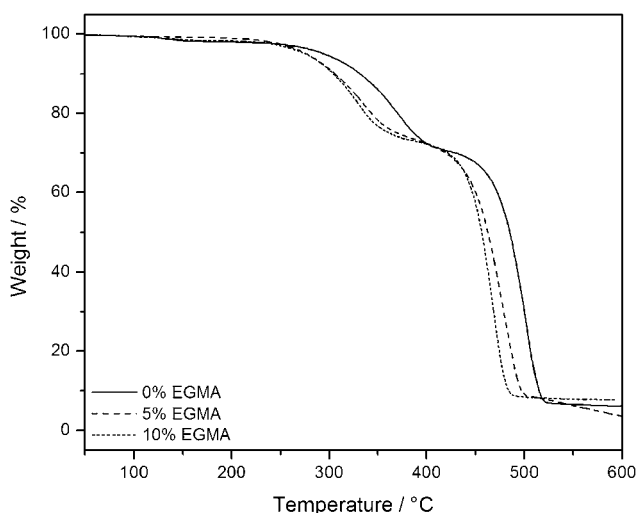


**Figure 10** TGA curves of composite samples.

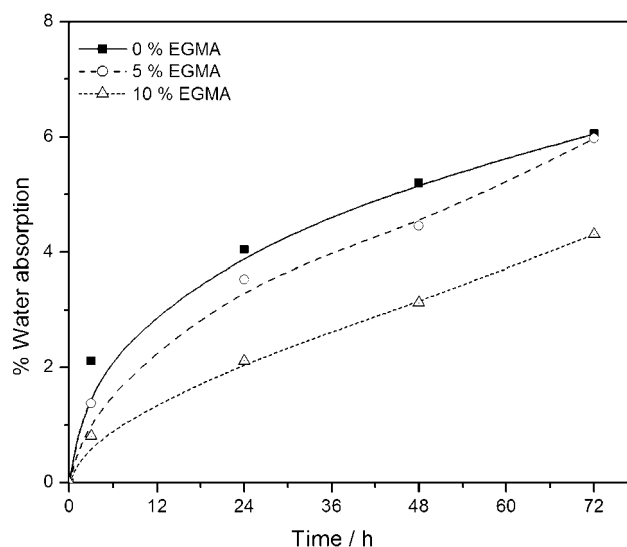


**Figure 11** Effect of EGMA content on the water absorption of composites with 25% WF ( $<150 \mu\text{m}$ ).

of the compatibilized composites. The 5% EGMA compatibilized composites have better thermal stabilities than the 10% EGMA compatibilized composites. This was expected because the presence of EGMA in EVA decreases the thermal stability of the matrix. It seems as if WF does not have a marked influence on the onset temperature of the second decomposition step in the absence of EGMA, while the onset temperature of decomposition of this step increases with increasing WF content when EGMA is present, although it is still lower than that of the uncompatibilized composites. This is probably because of the weaker interaction between EVA and WF, while the behavior in the presence of EGMA is in line with the postulated reaction between EGMA and WF and the resultant stronger interaction with EVA. The reduced stability of the samples containing EGMA is the result of the low thermal stability of EGMA.

The water absorption of the composites is shown as function of time in Figure 11. In general, the water absorption increases as filler loading increases, while the compatibilized composites absorb less water than the uncompatibilized ones. The reason for this is that WF is hydrophylic and porous and is likely to absorb water. However, EGMA grafting of WF causes more effective filling of the WF pores by matrix material, giving rise to reduced water absorption.

## CONCLUSIONS

IF there is an interaction between the  $-C=O$  of EVA and the OH groups of WF, it seems to be very weak, and the resulting composites have poor properties. The presence of EGMA in the composite improved most of the investigated properties because of the improved interaction between the

matrix and WF in the presence of EGMA. IR analysis shows that there is probably a reaction between the epoxy groups in EGMA and the —OH groups in WF, giving a grafted product. Through this grafting, it wets the WF surfaces and this further improves the interaction with the matrix material. The resulting composites have better properties than EVA or its uncompatibilized composites.

The amount of compatibilizer has an effect on the properties of the composites. The mechanical properties of 10% EGMA compatibilized composites are better than those of the 5% EGMA compatibilized composites. The 10% EGMA compatibilized composites are thermally less stable than the 5% EGMA compatibilized and uncompatibilized composites, because of the lower thermal stability of EGMA. Oxygen permeability and water absorption decrease with an increase of EGMA in the composites, because of the more effective penetration of the WF pores by the matrix material which is the result of the EGMA–WF grafting that occurs.

## References

1. Czviskovzky, T. *Radiat Phys Chem* 1996, 47, 425.
2. Bengtsson, M.; Oksman, K. *Compos A* 2006, 37, 752.
3. Bengtsson, M.; Gatenholm, P.; Oksman, K. *Compos Sci Technol* 2005, 65, 1468.
4. Vaino, M. H.; Heino, M.; Seppala, J. *Polymer* 1998, 39, 865.
5. Georgopoulos, S. T.; Tarantili, P. A.; Avgerinos, E.; Andreopoulos, A. G.; Koukios, A. G. *Polym Degrad Stab* 2005, 90, 303.
6. Gassan, J.; Gutowski, V. S. *Compos Sci Technol* 2000, 60, 2857.
7. Tserkia, V.; Zafeiropoulos, N. E.; Simon, F.; Panayiotou, C. *Compos A* 2005, 36, 1110.
8. Balasuriya, P. W.; Ye, L.; Mai, Y. W. *Compos A* 2001, 32, 619.
9. Oksman, K.; Clemons, C. *J Appl Polym Sci* 1998, 67, 1503.
10. Liao, B.; Huang, Y.; Cong, G. *J Appl Polym Sci* 1997, 66, 1561.
11. Maldas, D.; Kokta, B. V.; Raj, R. G.; Daneault, C. *Polymer* 1988, 29, 1255.
12. Oksman, K.; Lindberg, H.; Holmgren, A. *J Appl Polym Sci* 1998, 68, 1845.
13. Countino, F. M. B.; Costa, T. H. S.; Carvalho, D. L. *J Appl Polym Sci* 1997, 65, 1227.
14. Selke, E. S.; Wichman, I. *Compos A* 2004, 35, 321.
15. Ismail, H.; Jaffri, R. M. *Polym Test* 1999, 18, 381.
16. Salemane, M. G.; Luyt, A. S. *J Appl Polym Sci* 2006, 100, 4173.
17. Malunka, M. E.; Luyt, A. S.; Krump, H. *J Appl Polym Sci* 2006, 100, 1607.
18. Yang, H. S.; Kim, H. J.; Park, H. J.; Lee, B. J.; Hwang, T. S. *Compos Struct* 2006, 72, 429.
19. Espert, A.; Vilaplana, F.; Larlsson, S. *Compos A* 2004, 35, 1267.
20. Elvy, S. B.; Dennis, G. R.; Teck, L. *J Mater Process Technol* 1995, 48, 365.
21. Sedlakova, M.; Lacik, I.; Chodak, I. *Macromol Symp* 2001, 170, 157.
22. Heino, M. T.; Seppala, J. V. *J Appl Polym Sci* 1993, 48, 1677.
23. Chiou, Y. P.; Chang, D. Y.; Chang, F. C. *Polymer* 1996, 37, 5653.
24. Chiou, Y. P.; Chang, D. Y.; Chang, F. C. *Polymer* 1996, 37, 4099.
25. Miller, M. M.; Cowie, J. M. G.; Tait, J. G.; Brydon, D. L.; Mather, R. R. *Polymer* 1995, 36, 3107.